Journal of Aerosol Science 183 (2025) 106485

Contents lists available at ScienceDirect

Journal of Aerosol Science

journal homepage: www.elsevier.com/locate/jaerosci

Potential human exposure and risks of incidental nanoparticles released during rotary dry cutting of ceramic tiles

Verónica Moreno-Martín [a,b,*], Maria López [a], Cristian Roldan [h], David Bou [h], Sonia Fraga [d,e,f,g], João Paulo Teixeira [d,e,f], Ana López-Lilao [h], Vicenta Sanfélix [h], Raúl Moliner [h], Eliseo Monfort [h], Mar Viana [a,c]

[a] Department of Geosciences, Institute of Environmental Assessment and Water Research, Spanish Research Council, Carrer de Jordi Girona 18-26, Barcelona, 08034, Spain
[b] Barcelona University, Chemistry Faculty, Programa de doctorat de Química analítica i medi ambient, Carrer Martí i Franquès 1-11, Barcelona, 08028, Spain
[c] Spanish Ministry of Ecological Transition, Pollution Prevention Unit, Pza. San Juan de la Crus 10, 28071, Madrid, Spain
[d] Department of Environmental Health, National Institute of Health Dr. Ricardo Jorge, Rua Alexandre Herculano 321, Porto, 4000-053, Portugal
[e] EPIUnit-Institute of Public Health, University of Porto, Rua das Taipas 135, Porto, 4050-600, Portugal
[f] Laboratory for Integrative and Translational Research in Population Health (ITR), Rua das Taipas 135, Porto, 4050-600, Portugal
[g] Department of Biomedicine, Unit of Pharmacology and Therapeutics, Faculty of Medicine, University of Porto, Rua das Taipas 135, Porto, 4050-600, Portugal
[h] Institute of Ceramic Technology (ITC-AICE), Universitat Jaume I, Avinguda de Vicent Sos Baynat, s/n, Castelló de la Plana, 12006, Spain

A R T I C L E   I N F O

Handling Editor: Dr Miikka Dal Maso

Keywords:
Ultrafine particles
Clay
Rectify
Human exposure
Health and safety

A B S T R A C T

Rotary dry cutting and rectifying of ceramic tiles are sources of fine particulate matter (PM2.5) and nanoparticles (NPs). These activities are typically carried out inside industrial facilities during the manufacturing process, as well as outdoors and in residential indoor spaces during the installation phase, where mitigation measures are seldom implemented. This work aimed to understand the particle formation and release mechanisms, as well as particle properties (physical, chemical, and toxicological) and potential impacts on human health and the environment, for particles generated during ceramic tile rotary dry cutting operations. Aerosols were characterised in terms of particle number and mass concentrations, chemical composition, morphology and *in vitro* cytotoxicity. Two types of commercially available and representative tiles were tested in controlled chamber experiments: porous and non-porous ceramic body tiles (referred to in this work as A and B types, respectively). Results evidenced the release of fine particles and NPs during dry cutting of both materials, in comparable concentrations (20.000–45.000/cm^3, 1-min average). However, the particle size distribution was significantly finer from A tiles (70% of the particle number concentration was nanosized (<100 nm)) in comparison to B tiles (<20%). While airborne particle chemical profiles were similar for both types of materials in the coarser size fractions (>0.6 μm), in the smaller size fractions (<0.6 μm) larger differences were observed. The chemical composition of airborne aerosols was consistent with that of the deposited dust. *In vitro* cytotoxicity responses evidenced statistically significant differences between exposure to aerosols from both types of tiles: cell viability was lower after exposure to aerosols from A tiles (50% at the original concentration) compared to those from B tiles, which exhibited high cell

* Corresponding author. Department of Geosciences, Institute of Environmental Assessment and Water Research, Spanish Research Council, Carrer de Jordi Girona 18-26, Barcelona, 08034, Spain.
E-mail address: veronica.moreno@idaea.csic.es (V. Moreno-Martín).

https://doi.org/10.1016/j.jaerosci.2024.106485
Received 23 May 2024; Received in revised form 1 October 2024; Accepted 1 November 2024
Available online 2 November 2024

viability regardless of the aerosol concentration. Overall, results evidenced NP formation and release during rotary dry cutting of ceramic tiles, varying physical-chemical and cytotoxic profiles as a function of the material being processed, and highlight this activity as a potential health hazard in scenarios where prevention and mitigation measures are not implemented.

1. Introduction

The physical properties of ceramic materials (eg., durability, strength, non-corrosiveness, high-temperature resistance) render them highly valuable in e.g. enamels, abrasives and refractories and in critical industrial processes such as construction, metallurgy and glass production (Pampuch, 2014). With a total turnover of €26 billion within the European Union (EU), this industrial sector provides over 200.000 direct jobs and 400.000 indirect jobs across all countries in Europe (Cerame Unie, 2021).

Typical activities linked to ceramic products, whether during their manufacture or installation (e.g., from tiling of walls in indoor microenvironments to outdoor pavements), involve cutting, drilling, sawing and grinding. These high-energy machining activities, when carried out using dry methods, generate incidental aerosol emissions, ranging from coarse (>10 μm) to ultrafine and nanoparticles (<100 nm) (Bessa et al., 2020; Ribalta et al., 2019a; Salmatonidis et al., 2018, 2019, 2020; Viana et al., 2017; Viitanen et al., 2017). Key chemical tracers in these aerosols are Si, Zr, Ti, Sn, Al, Cu or Cr (Fonseca et al., 2015a). The activities described above generate incidental emissions of with well-known health impacts (Lelieveld et al., 2015; Oberdörster, 2001; Pope III & Dockery, 2006). Particles are typically generated in indoor or outdoor air, as a function of the activity (manufacture, handling, packaging, installation or removal), resulting in potential environmental and human health impacts. In addition, recycling and waste disposal of used ceramic tiles are also potential sources of environmental release when involving high-energy operations such as grinding. Due to the large variety of applications (from industrial to household) and their scale (from industrial manufacture to individual installation) aerosols released during the ceramic tile value chain may exert major potential impacts on human health and the environment (Hall et al., 2013).

The generation and release have been studied for a significant number of processes (in the ceramic industry), including handling of ceramic bulk materials, laser sintering of tiles, thermal spraying of ceramic coatings and laser cladding (Bramming Jørgensen & Teresia Kero, 2017; A.S. Fonseca et al., 2015; A. S. Fonseca et al., 2015b, Fonseca et al., 2015; Hossain et al., 2023; Lovén et al., 2023; Ribalta et al., 2019a; Salmatonidis et al., 2019; Viana et al., 2017; Voliotis et al., 2014; Balout et al., 2007). The literature focuses mostly on aerosol emissions and exposure impacts generated in industrial environments, where mitigation measures (e.g., localised, general exhaust ventilation systems and personal protective equipment) may be easily implemented and their efficiency quantified (Salmatonidis et al., 2019). Examples of mitigation measures are wet machining work, use of low-speed saws, general ventilation and local extraction systems or cleaning the work area by wet methods or aspiration (Rakshit & Das, 2019). Conversely, installation of ceramic materials is commonly carried out outside industrial facilities (on construction and building sites, in households and other private/commercial indoor or outdoor microenvironments), where mitigation measures are reported to be scarce in some cases (WHS, 2023) resulting in environmental and human exposures.

Different techniques can be used to cut ceramic tiles (Aparicio Sanchez & Baena Molina, 2013; Rakshit & Das, 2019; Xu et al., 2023). Manual tile scribes and tile cutters are frequently used, which score the tiles with a tungsten carbide tip (tiles scribe) or with a glaze diamond tipped wheel (tile cutters) before snapping the tile. This technique is fast and simple and much less dusty than rotary cutting procedures (Garcia et al., 2014; Hall et al., 2013). However, some materials cannot be cut by means of this procedure because of their hardness and/or thickness. Additionally, these tools only allow to cut straight lines. Laser cutting or waterjet tile cutting can be used instead for cutting complex or intricate shapes and designs (Black & Chua, 2017; Krajcarz, Bańkowski, & Młynarczyk, 2017). For larger projects where a variety of cuts are required, electric rotary cutter machines, including angle grinders, are usually used. Because ceramic-tile cutting using these machines can generate high aerosol emissions they may be equipped with preventive (e.g.: low-speed rotation) and corrective measures (such as vacuum cleaners or wet cutting, if water supply is available). As a result, real-world scenarios are expected to be highly variable and complex, where a combination of the different technologies may be used, depending on professional or do-it-yourself use, level of training, material processed, etc.

In this framework, this work aimed to deeply understand the potential human health impacts posed by aerosols generated during rotary dry cutting of ceramic tiles. The simulation was designed to represent a worst-case scenario such as the installation of tiles an indoor or outdoor environment, and therefore without local exhaust ventilation. To this end, incidental aerosol release was simulated in an experimental chamber, and the physical, chemical, morphological and toxicological properties of the aerosols (10 nm - 10 μm) were characterised. Results aimed to provide insights into the potential human exposure and risks from tile cutting aerosols. Moreover, results obtained may be partially extrapolated to the end-of-life activities involving high-energy operations, such as ceramic tile crushing, grinding or machining for recycling or waste disposal (e.g., in demolition sites, landfills, etc.; Bolyard et al., 2013; Duan et al., 2017; Martínez et al., 2021), where the relevance of exposure to mixed types of dust has been reported (De Ipiña et al., 2015).

2. Materials and methods

2.1. Experimental chamber and instrumentation

Ceramic tile cutting simulations were carried out in an experimental chamber at the Institute of Ceramic Technology (ITC-AICE) in

Castellón, Spain. The test booth is a cabin connected through a funnel (Fig. 1; 3) to a circular duct (Fig. 1; 4) equipped with a fan and a HEPA filter located at the entry of the booth. The fan generates an airflow inside the testing both, from the inlet towards the funnel, achieving a uniform velocity across the cross-sectional area of the both. The average air velocity in the testing both (1) is determined based on the selected flow rate (Q) (regulated to remain constant throughout the test), considering that it must be capable of transporting the respirable particles emitted from the emission source to the sampling section. The flow rate used was 52.5 m^3/min. The particle concentrations can be measured at the sampling section (Fig. 1) of the conduct or, alternatively, at the booth (using direct-reading instruments). The sampling carried out in the sampling section was isokinetic and the duration of the measurement should be sufficient to acquire representative concentration data and aerosol mass sampled for subsequent analysis.

The cutting instrumentation (TC-125, Rubi, Spain) was fixed on a table at the centre of the chamber (Fig. 1), at a 0.5m distance (near field) from the monitoring instrumentation. The rotating saw was manually controlled by an operator wearing the necessary personal protective equipment (FFP3, protective glasses, earplugs and gloves).

The aerosol monitoring instrumentation was placed at two sampling locations simultaneously, on the testing booth (TB) and in the sampling conduit (sampling section; SS) (Table 1). At each of these sampling locations the concentrations of inhalable, respirable, and nanometric particle fractions were continuously monitored, and in addition samples were collected for subsequent chemical, morphological and toxicological characterisation.

2.2. *Ceramic materials tested*

Depending on the formation method and body porosity (determined by water absorption), ceramic tiles can be classified in different groups according to international standards. In this study two different types of commercial glazed ceramic tiles (after firing, ready for commercial use) were tested. The main characteristics of the studied tiles are summarised in Table 2.

2.3. *Aerosol monitoring, sampling and characterisation*

Online instrumentation: particle number concentrations (N), mass concentration, size distribution and mean diameter (Dp) were monitored with online instrumentation (Table 1).

- Electrical mobility spectrometer NanoScan SMPS (TSI Model 3910, USA), monitoring particle number size distributions from 10 to 420 nm, in 13 channels with 1-min time resolution.
- Mini laser aerosol spectrometer Mini-LAS 11-R (Grimm, Germany), for total and size-segregated particle mass concentrations between 0.25 and 32 μm (monitoring inhalable, thoracic and respirable dust, particle mass and number concentration), in 31 channels with 6 s time resolution.

In addition, physical, chemical and toxicological properties of aerosols were determined on samples collected using different sampling techniques:

Chemical properties: size-resolved aerosol chemical composition was determined after sample collection on polycarbonate filters with an Electrical Low-Pressure Impactor (ELPI+) (Dekati, Finland), ranging from 6 nm to 10 μm in 15 stages (Table S1). The chemical composition was determined by acid digestion of the filters and analysing the resulting extract for major and trace elements by inductively-coupled plasma atomic-emission spectrometry (ICP-AES, Thermo Fisher Scientific, model iCAP 6500 Radial) and inductively-coupled plasma mass spectrometry (ICP-MS, model iCAP-RQ, Thermo Fisher Scientific, USA) (Querol et al., 2001.). In cases which the sample mass on each individual filter was insufficient for separate analysis, multiple filters were digested in the same batch (together) for ICP analysis. Major components were expressed as oxides and SiO_2 concentrations were estimated indirectly from Al_2O_3 concentrations, using a factor of 2.8 (SiO_2/Al_2O_3) (Barba, 2002). In addition, the deposited dust in each experiment was collected from the cutting table using a brush; these samples were chemically treated by acid digestion of 0.10g of sample following the method proposed by Querol, Whateley, Fernfindez-Turiel, & Tuncali (1997) and subsequently analysed by ICP-AES and ICP-MS.

Single particle morphology and composition: the morphology and composition of single particles was analysed by Scanning

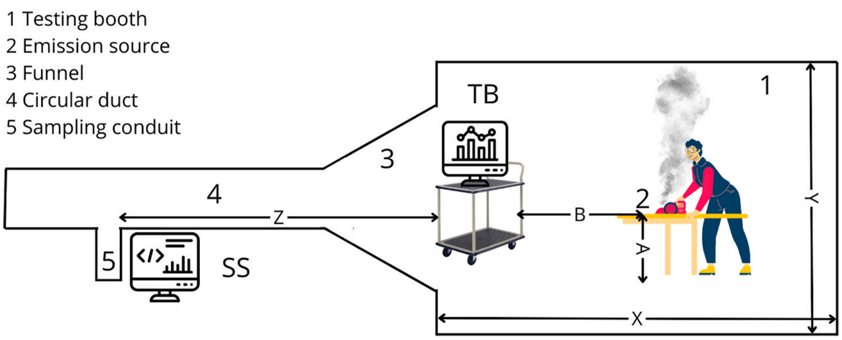

Fig. 1. Testing booth scheme. Dimensions: X = 3m, Y = 3m, A = 1m, B = 0.5m Z = 3m.

Table 1
Location and key parameters of the instrumentation deployed during the experiments. TB=Testing Booth, SS= Sampling section conduit.

Instrumentation	Particle size range	Parameter	Location
NanoScan SMPS (TSI Inc., Model 3910)	10–420 nm	Particle size distribution	TB
Mini-LAS 11R (Grimm Aerosol Technnik, Germany)	0.25–32 μm	Particle mass concentration	TB
Electrical Low Pressure Impactor (ELPI+)	6 nm–10 μm	Chemical characterisation	SS
BioSampler (SKC)	PM_2	Cytotoxicity	TB
SEM grids (Quantifoil) (SKC)	–	Morphology	TB

Table 2
Characteristics of the ceramic tiles studied.

Reference in the study	A	B
Group (ISO13006- UNE-EN 14411)	BIII	BIa
Surface finish	Glazed	Glazed
Body type	Earthenware	Porcelain
Water absorption (% by weight)	11–15	<0.5
Surface dimension (cm*cm)	30*30	30*60
Thickness (mm)	12	20
Typical use	Wall tiles Indoor	Floor tiles and countertops Indoor and outdoor

Electron Microscopy (SEM) (QUATTRO S, Thermo Fisher Scientific, USA) microscope coupled with an energy-dispersive X-ray (EDX) spectrometer (Pathfinder, Thermo Fisher Scientific, USA). Particles were collected on SEM grids Quantifolil® AU grids with 1 μm diameter holes – 4 μm separation of 200 mesh) placed in sampling cassettes (SKC INS, USA, inlet diameter 1/8 in, filter diameter 25 mm) following the sampling set up described by Tsai et al. (2009), Fonseca et al. (2015) and Ribalta et al. (2019a). The cassettes were connected to an SKC Leland pump (3 l/min). Samples for morphological assessment were collected inside the testing booth.

PM_2 sampling for in vitro testing: PM_2 aerosol samples were collected using an SKC BioSampler® connected to a sonic-flow BioLite + pump (12.5 l/min) over 30 min. The particles were collected in 20 ml-glass vessels containing serum-free DMEM (Dulbecco's modified Eagle's medium) with 100U/ml of penicillin and 100 μg/ml streptomycin (100 μg/mL) to avoid the proliferation of bacteria. Samples were conserved frozen in 50 mL falcon tubes at −20 °C until analysis.

In vitro testing of PM_2 liquid suspensions. The potential effect of the particles sampled on the viability of human alveolar epithelial A549 cells (American Type Culture Collection) was assessed by the Alamar Blue (AB) assay, as previously described (Davoren et al., 2007), with minor modifications(López et al., 2022). Cells were cultured in DMEM (Gibco-Thermo Fisher Scientific, USA) supplemented with 10% FBS (Gibco-Thermo Fisher Scientific, USA), 100/mL penicillin and 100 μg/mL streptomycin (Gibco--Thermo Fisher Scientific, USA) and maintained in a humidified cell incubator at 37 °C with 5% CO_2. To carry out the cytotoxicity experiments, cells were seeded in 96-well plates (150000 cells/well) and allowed to adhere for 48 h at 37 °C and 5% CO_2. A total of 4 samples were collected (2 per material), and cell viability was tested for the original aerosol concentration as sampled inside the chamber, as well as two subsequent dilutions (1:2 and 1:4). The submerged cultures were exposed for 24 h to the original suspension (1x) and to different dilutions of the airborne particle liquid samples (1:2 and 1:4). Cells incubated with serum-free DMEM served as negative control (NC), whereas cells exposed to 70% ethanol (EtOH) served as positive control (PC). After exposure, the medium was aspirated and 100μl/well of AB reagent diluted to 1:10 were added for a 3 h at 37 °C and 5% CO_2. After incubation, fluorescence was measured in a microplate reader (Molecular Devices SpectraMax® iD3, USA) at an excitation wavelength of 570 nm and emission at

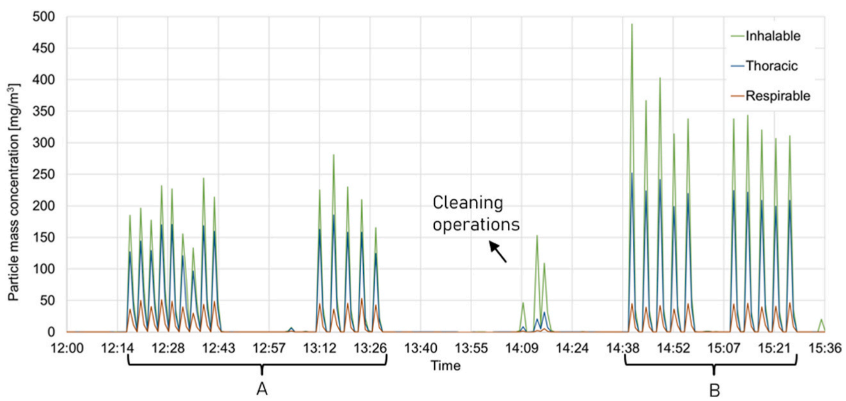

Fig. 2. Particle mass concentrations (mg/m^3) recorded in the testing booth during the experiments. Chamber cleaning operations are indicated.

610 nm. Data was normalised considering the NC mean value and expressed in percentage of NC. For each sample, three technical replicates were measured.

2.4. Experimental design

Particle mass and number concentrations and size distribution were monitored during 4 different experiments with the full experimental set up described in Table 1. In addition, experiments were reported with a simplified set up (using DiscMini particle counters for particle number concentration and mean particle size), with comparable results (reported in Supporting Information). The data obtained during these experiments were also crucial in the configuration of the full set up.

During each experiment (two per type of product), the operator manually performed a minimum of five cuts with a duration of 1 min of active cutting at a cutting feeding speed of 1 cm/s, leaving 2 min between active cuts. The ventilation system was continuously working, facilitating the data treatment as separate peaks, corresponding to each active cutting period (Fig. 2).

2.5. Statistical analysis

Different methods were applied to assess the statistical significance of scenarios and samples. For the on-line data, the NanoGEM approach was employed to identify statistically significant increases in particle number concentrations (Asbach et al., 2012). While NanoGEM approach was originally designed and validated for particle number concentrations, and it was subsequently also validated for particle mass concentrations (Ribalta et al., 2019a). In addition, the normality of the data was analysed by Kolmogorov-Smirnov test (using SPSS statics 27). In case of normal distribution of the data, the parametric ANOVA test was performed to assess the significance of the datasets, while for the non-parametric data the Kruskal-Wallis test was applied.

Finally, statistical and nonlinear regression analyses of cytotoxicity data were performed using GraphPad Prism 6 (GraphPad Software, Inc., USA). The half-maximal inhibitory concentration (IC_{50}) values of the PM_2 liquid samples were estimated from the AB concentration-response curves, fitted using a three-parameter log (inhibitor vs. normalised response model) using the least squares as fitting method. Significance was accepted at a P value < 0.05.

3. Results and discussion

3.1. Fine and coarse aerosol generation and release

Fine and coarse particle mass concentrations generated were monitored during cutting of tiles A (experiments 1 and 2) and B (experiments 3 and 4). Monitoring was carried out in 3 size fractions: inhalable, thoracic and respirable (Table 3; and results from the simplified set up in Supporting Information). Mean background concentrations (pre-activity) for the inhalable, thoracic and respirable fractions were 30, 20 and 15 μg/m^3, respectively. As anticipated, particle mass concentrations increased notably during cutting. Previous studies reported the release of particulate matter (PM) during activities involving cutting, drilling, and crushing of silica-containing materials (Carlo et al., 2010; Garcia et al., 2014; Hall et al., 2013). All experiments displayed a similar profile, characterised by clear peaks and relatively uniform values, marked by intermittent activity and air renewals (Fig. 2). On average, mean concentrations of the inhalable, thoracic and respirable size fractions measured in the testing booth were of the same order of magnitude (no statistical differences according to ANOVA) during cutting of A tiles (inhalable = 72.0–88.6 mg/m^3; thoracic = 50.8–63.1 mg/m^3; respirable = 14.6–18.8 mg/m^3) and B tiles (inhalable = 100.4–117.7 mg/m^3; thoracic = 66.8–71.5 mg/m^3; respirable = 14.2–14.7 mg/m^3).

The mean respirable fraction obtained during the active cutting (14–19 mg/m^3) exhibited lower concentrations to those registered in certain studies (39.2 and 49.7 mg/m^3 for cutting s-shape and flat-concrete roofing tiles respectively, a masonry circular saw (Carlo et al., 2010) and slightly higher than those registered in some studies (7.2–12.6 mg/m^3) in which the emissions related with the cutting of natural and artificial stone are cut with similar tools(Hall et al., 2022). However, it should be noted that comparisons between chamber studies are not always direct due to differences in the experimental design (ventilation rates etc.). In spite of this, the results and literature evidence that the formation and release of fine and coarse PM during rotating dry cutting of tiles is relevant in terms of human exposure, if no effective mitigation measures are implemented. Furthermore, when carried out in outdoor air, these activities also constitute a potential source of ambient air pollutants.

Table 3
Fine and coarse aerosol concentrations recorded during the different experiments; DL: detection limit.

PM fractions	Inhalable (mg/m^3)			Thoracic (mg/m^3)			Respirable (mg/m^3)		
Tile	Avg.	Max.	Min.	Avg.	Max.	Min.	Avg.	Max.	Min.
A (E1)	89	244	1	63	170	0.9	19	51	0.3
A (E2)	72	281	<DL	51	185	<DL	15	53	<DL
B (E3)	118	488	0.1	72	252	0.1	15	45	<DL
B (E4)	100	343	0.2	67	224	0.1	14	46	<DL

3.2. Nanoparticle generation and release

In addition to fine and coarse aerosols, nanoparticle formation and release were evidenced in all of the experiments. As observed for micron-sized particles, the different experiments displayed NP emission trends, characterised by clear peaks and relatively uniform maximum concentrations, marked by intermittent activity and air renewals (Fig. 3). The results from the simplified set up, when total particle number concentrations were monitored instead of aerosol size distributions, were comparable and are reported in Supporting Information.

Based on NanoGem approach; (Asbach et al., 2012), NP concentrations during tile cutting were statistically different from background concentrations. Nanoparticle concentrations in the chamber were mostly consistent across all experiments (Exp 1: 21834/cm^3, Exp2: 33780/cm^3, Exp3: 35120 and Exp 4: 26957/cm^3) irrespective of the type of tile being cut (Table 4). These concentrations were lower than those reported in other studies dealing with ceramic activities: Voliotis et al. (2014) characterised NPs emitted during unglazed and glazed ceramic tile firing (thermal process) in a traditional small-sized pottery studio, obtaining average particle number concentrations of 1 × 10^5/cm^3 and 2.5 × 10^5/cm^3. A different study (Fonseca et al., 2015b) assessed the ultrafine and NP formation and emission mechanisms during laser ablation of ceramic tiles (thermal process), finding concentrations up to 2.6 × 10^6/cm^3. In 2016, the same authors (Fonseca et al., 2016) also identified NP formation and release mechanisms and their impact on exposure during tile sintering (up to 1 × 10^7/cm^3, thermal process), while other researchers (Viana et al., 2017) evaluated workplace exposure to NPs during atmospheric plasma spraying (thermal process) in the ceramic industry (up to 3.3 × 10^6/cm^3) inside the spraying chamber and on the worker area (up to 8.3 × 10^5/cm^3). Finally, Ribalta et al. (2019b) evaluated personal exposure to particles and dustiness during handling of powders in industrial ceramic settings (mechanical process) concluding that NPs may have a potential impact on worker exposure (from 9179/cm^3 to 51461/cm^3, depending on the material). Other studies (Salmatonidis et al., 2018) reported high NP concentrations released during pulsed laser ablation (thermal process) of ceramic tiles (up to 2.7 × 10^6/cm^3). In sum, NP concentrations reported in this work, which studies a mechanical process of cutting (2.2 × 10^4 to 3.5 × 10^4/cm^3), were much lower than those reported during ceramic thermal processes (>10^5/cm^3), but comparable with those reported in other mechanical processes of the ceramic industry (9 × 10^3 to 5 × 10^4/cm^3).

Regarding particle size distribution, a bimodal size distribution for both types of tiles was observed (Fig. 4), showing higher NP concentrations (8365-7210/cm^3; 37-27 nm) for A tiles than for B tiles (2704–2943/cm^3; 15 nm) in the smallest mode. Specifically, 70% of the ultrafine particles emitted when cutting A tiles was <100 nm (with 10% having mean diameter <50 nm), whereas for B tiles the percentage of particles <100 nm was lower than 20% (Fig. 4). These results evidence major differences between aerosol size distributions from the two types of tiles assessed.

3.3. Aerosol size-resolved chemical fingerprint and morphology

Size-resolved chemical composition of aerosols generated during rotating dry cutting of A and B tiles were characterised in terms of their major and minor components. Major components were comparable in the coarser aerosol fractions (>0.605 μm) for both types of tiles. As expected, ceramic components were the major constituents of aerosol mass: SiO_2 contributed with the largest proportion (50–55%) of >0.605 μm aerosols, followed by Al_2O_3 (20–21%), CaO (9–10%), and Fe_2O_3 (3–6%). Conversely, certain differences were observed in the smaller aerosol fractions (<0.605 μm) between both types of tiles, with a larger contribution from SO_4^{2-} in the smaller aerosols emitted by A tiles (up to 52% of the 0.156 μm fraction). For B materials, a larger contribution from Na_2O (12%) was detected in aerosols <0.257 μm (Fig. 5). In the field of ceramics and glass technology it is common practice to express chemical analyses and molecular formulas in terms of their oxide equivalents. While this is convention it is also simplification, as these oxides do not necessary represent the actual compounds present in raw materials or finished products such as glazes and frits.

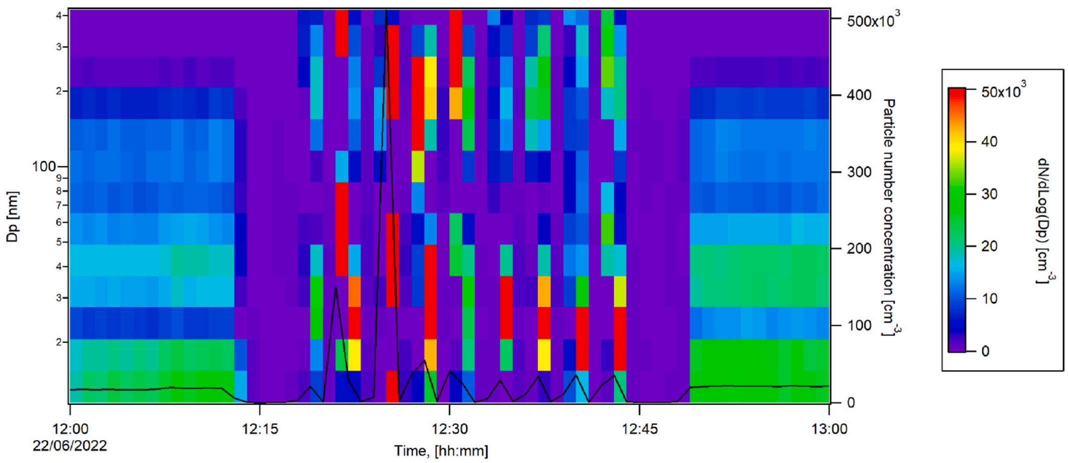

Fig. 3. Nanoparticle release during experiment 1 (Tile A). Particle diameter (Dp) in logarithmic scale.

Table 4
Mean NP number concentrations and diameter monitored throughout the different experiments. E: Experiment.

Experiment		E1	E2	E3	E4
Tile		A	A	B	B
N(cm^{-3})	Avg.	21834	33784	35123	26957
	Max.	286486	510765	149288	85504
	Min.	196	269	4187	2074
	P90%	30982	41032	94704	60556
	Avg.	84	103	184	182
Dp (nm)	Max.	173	219	253	230
	Min.	36	219	22	78
	P90%	132	174	235	228

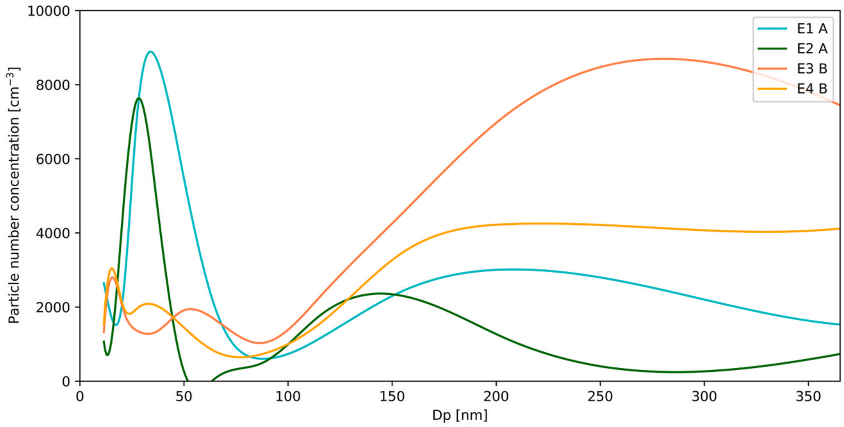

Fig. 4. Particle size distribution for aerosols emitted during the A and B tile cutting experiments. E: Experiment.

In terms of trace components, the size resolved chemical profiles demonstrated again similarities between both types of materials: the Ti content increased with particle size, while the Cr content decreased (Fig. 6). Coarser aerosol fractions (>0.605 µm) were also comparable for both types of tiles. Contributions were dominated by Ti (40–55%), followed by Ba (10–15%) and Sr (3–4%) except for 2.480 µm of B aerosols, where the contribution from Sr was larger (12%) than in A tile. Differences were observed once again in the smaller fractions: for 0.384 µm particles the primary component of A aerosols was Zn (47%), while for B aerosol it was Ti (33%). In the 0.257 µm fraction, higher percentages of Cr (23%) and Ni (16%) are observed in A aerosol, whereas for B materials Ti (31%) remained the major component. Finally, the primary aerosol component of 0.156 µm A aerosols was Ni (45%), while Cr (40%) dominated in B aerosols. These differences probably sourced from the difference in the glazes and pigments used, as well as impurities.

Comparable results were obtained for deposited dust (reported in Supporting Information).

In terms of particle morphology, assessed by scanning electron microscopy (SEM), aerosols released from both materials exhibited irregular morphologies, with a broad spectrum of sizes and agglomerates covering from nanoparticles to coarse aerosols (Fig. 7). This is consistent with conventional cutting techniques, such as diamond saw dry cutting, as this technique is unable to produce damage free cuts because the cutting force induces micro cracks on the surface and edge chipping (Rakshit & Das, 2019; Salmatonidis et al., 2018). Most of the particles showed diameters <10 µm and were fundamentally constituted by Si, Al, Ca, Mg, K, Na and Fe, consistent with the results described in the previous section. A large proportion of silica particles was observed. The similarity between both samples probably implies that the main parameter controlling particle morphology was the actual cutting process, with the tile composition having a lower influence on the morphology of the aerosols released. Unexpectedly, no significant difference was observed between the two studied ceramic tiles.

3.4. *Aerosol In vitro cytotoxicity testing of PM_2 liquid suspensions*

In view of the similarities observed between tiles in terms of coarse particle concentrations and major composition and the differences in terms of nanoparticle size distribution and key tracers, cellular viability was assessed after cell exposure during 24h to PM_2 aerosols collected in serum-free DMEM (Fig. 8). Samples collected during A-tile cutting (E1 and E2) significantly reduced human alveolar epithelial cell viability, dropping to 49.1% (E1) for the original (as collected) PM_2 liquid suspension. The samples collected during B-tile dry cutting (E3 and E4) did not significantly change the cell viability, which ranged between 88.5% and 98.6%, irrespective of their concentration. In the case of the liquid suspensions of the A aerosols, cell viability was lowest (49.2% for E1 and 68,9%

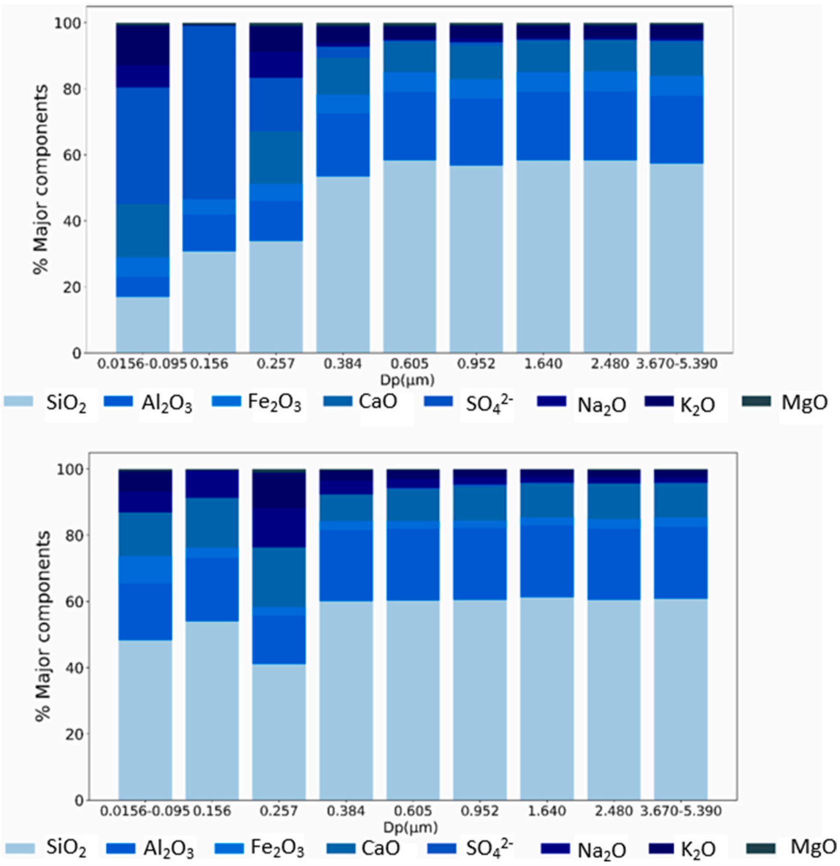

Fig. 5. Size-resolved relative chemical composition of aerosols sampled using an ELPI + impactor (14 stages), on polycarbonate impaction plates. *Filters corresponding to 0.0156-0.095 and 3.670-5.*390 µm *were digested together for ICP analysis, as the sample mass on each individual filter was insufficient for separate analysis*. Top: A aerosol release; bottom: B aerosol release.

for E2) with the highest particle concentration and it increased up to 93.9% when the 1:4 dilution was applied to the samples. Conversely, cell viability ranged between 88.5% and 99.2% for both samples of B aerosols, irrespective of their concentration. These patterns were consistent for both replicas of the A and B samples.

Results evidenced statistically significant differences between the cytotoxic response induced by the PM_2 released during cutting of the two different types of tiles, indicating that exposure and potential health risks derived from tile-cutting operations are dependent on the type of material being processed. The results discussed in the previous sections evidenced similarities between cutting of both types of tiles in terms of particle mass and number concentrations generated. However, differences were observed in terms of particle size distribution and relative contribution of certain inorganic tracers to the finer aerosol fractions. Given that particle size distribution results showed a larger proportion of nanoparticles emitted by A materials than from B (70% of total particle number in the case of A tile cutting vs. <20% for B), results suggest that the presence of NP may be associated with the decrease in cell viability in A samples. However, it is important to highlight that the use of PM_2 fraction for toxicity testing presents inherent challenges, as PM_2 encompasses both micron-sized and submicron particles. This broad classification makes it difficult to definitively link the reduction in cell viability observed with A tiles to the presence of nanoparticles alone. Previous studies demonstrated that ultrafine particles induce greater inflammatory response compared to fine particles (Oberdörster, 2001). Other researchers (Rafieepou et al., 2023) found that at concentrations exceeding 100 µg/ml, the cytotoxicity of SiO_2 nanoparticles is higher than that of microparticles. However, the chemical composition of the finer aerosol fractions, as shown in Fig. 5, may also influence cell viability: It is important to highlight here that the samples collected using the Biosampler refer to PM_2 aerosols, distinct from UFP or NPs (<100 nm). Consequently, the aerosol size fractions discussed in this section cannot be directly compared to the ones described in the sections above. Further research is necessary to understand the drivers of cell viability after exposure to PM_2 samples.

Finally, concentration–response curves were fitted using a three-parameter log (inhibitor vs. normalised response model). The IC50 (half-maximal inhibitory concentration), which indicates the concentration of particles needed to inhibit a biological process by half and is widely used as the experimental standard (Sebaugh, 2011), was calculated for A-type particles derived from tile cutting (Table 5), while for B particles it could not be calculated because of the low effect of the particles in the cells. This aligns with previous research (Ivask et al., 2015), which demonstrated that some heavy metal nanoparticles (CuO, ZnO, Sb_2O_3, Mn_3O_4, Co_3O_4) showed toxicity at nominal concentrations below 100 µg/mL in mammalian cells, with 24-h IC50 values ranging from 10 to 100 µg/mL.

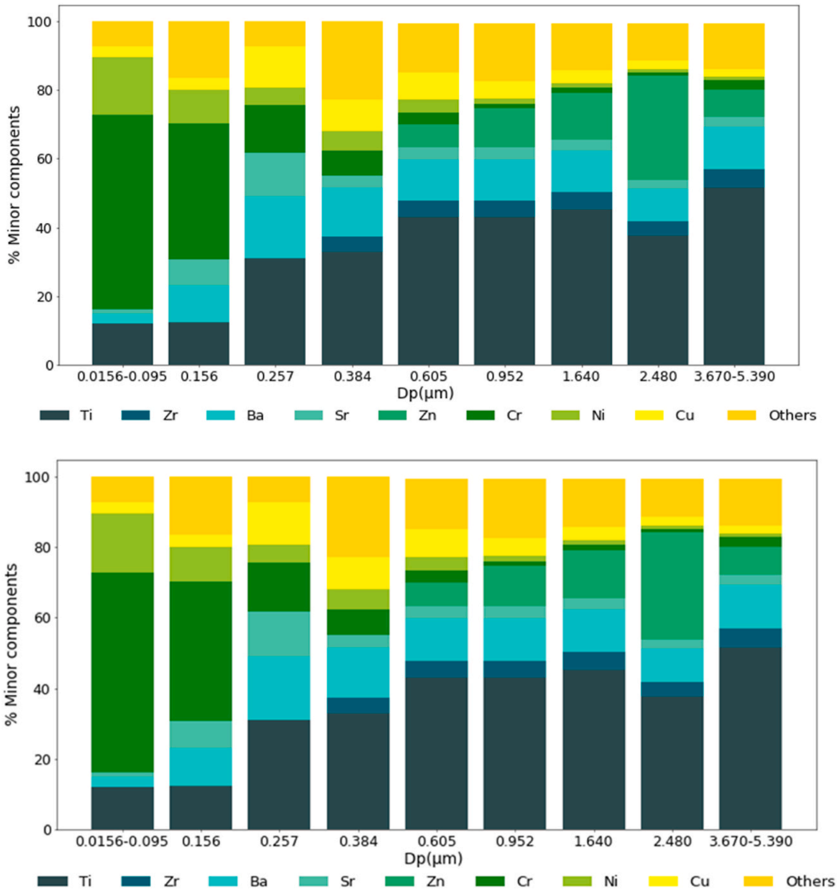

Fig. 6. Relative size-resolved chemical composition (trace elements) of aerosols sampled using an ELPI + impactor (14 stages), on polycarbonate impaction plates. Filters corresponding to 0.0156–0.095 and 3.670–5.390 µm were digested together for ICP analysis, as the sample mass on each individual filter was insufficient for separate analysis. Top: aerosols released from A tiles; bottom: aerosols released from B tiles.

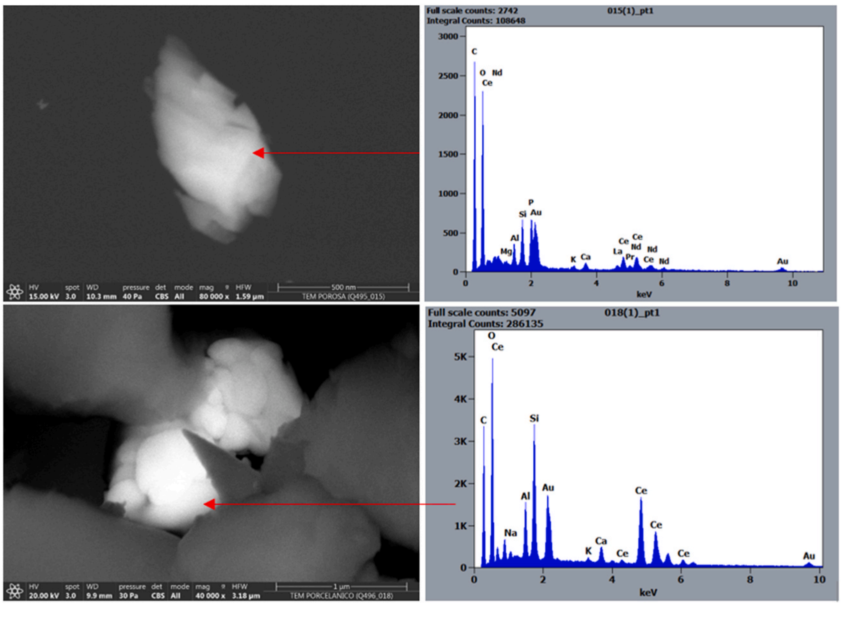

Fig. 7. Ceramic aerosol particles from A (top) and B (bottom) tiles.

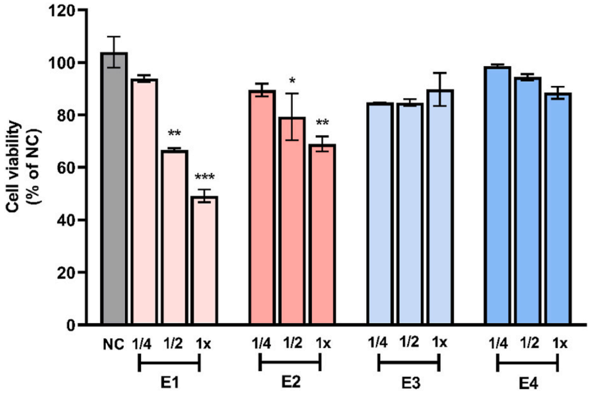

Fig. 8. Human alveolar epithelial cells viability (% of negative control; NC) after exposure for 24h to PM_2 fractions collected during two independent experiments of rotary dry cutting of tile A (E1 and E2) and tile B (E3 and E4).

Another study (Tokgun et al., 2015), revealed that SiO_2 NPs produce significant cytotoxicity to A549 cells in dose- and size-dependent manner, especially 6 nm with an IC50 value of 119.82 µg/ml. This suggests that the differences in the smaller fractions of the aerosol may contribute to the distinct cytotoxic responses.

Moreover, these differences in cell viability may not only stem from variations in the finer particle size distribution but also from the distinct chemical composition of the glaze, frits or raw material used in the tiles. It is important to note, however, the sampled fraction is PM_2, which includes both submicron and micron particles, and there are inherent limitations in fully attributing the observed effects solely to nanoparticles or their composition. Further research is necessary to disentangle these complex interactions.

4. Conclusions

Nanoparticle formation and release during rotary dry cutting of ceramic tiles was assessed in an experimental chamber. The main goal was to understand the potential human health impacts from this activity, under representative exposure concentrations. Two types of commercially-available, ceramic tiles were tested. Results evidenced that particle mass and number concentrations increased substantially during the cutting operations, with comparable concentrations released from both types of tile materials. Particle morphology for fine and coarse aerosols, determined by electron microscopy, also evidenced similarities between both types of tiles. However, statistically significant differences were observed in terms of nanoparticle emissions and chemical properties. Whereas nanoparticle release was evidenced during all of the tile cutting operations, 70% of total particle number concentrations released from A-type tiles were <100 nm, in contrast with less than 20% from B-type tiles. The chemical profiles of airborne particles and of deposited dust also showed differences between both types of tiles for aerosols <0.6 µm, while the composition of coarser fractions was mostly similar. Finally, *in vitro* toxicity tests reported statistically lower cell viability for A tile PM_2 fraction (decreasing to 49.1% at the exposure concentration) when compared to B PM_2 fraction, which exhibited high cell viability regardless of the concentration tested. Thus, it was concluded that the different toxicological responses obtained from A-tile and B-tile PM_2 fraction may be linked to the presence of NP, either because of the differences in size distribution and/or of differences in chemical composition of the lower size fractions (<0.6 µm).

In sum, this work identifies ceramic tile rotary dry cutting as a potential human health hazard under conditions when prevention measures are not implemented. Whereas effective mitigation measures are frequently used in industrial scenarios, this is not always the case during tile installation in indoor, residential or outdoor settings. In these cases, the use of effective mitigation measures should be strongly recommended.

Table 5
Half-maximal inhibitory concentration (IC_{50}) values of the PM_2 liquid suspensions obtained by the Alamar Blue (AB) viability assay concentration-response curves obtained in human alveolar epithelial cells after 24 h of exposure.

	E1-A	E2-A	E3-B	E4-B
Original suspension concentration (particles/mL)	7.27×10^{11}	3.23×10^{11}	9.83×10^{11}	4.76×10^{11}
1/2 suspension concentration (particles/mL)	3.65×10^{11}	1.65×10^{11}	4.92×10^{11}	2.38×10^{11}
1/4 suspension concentration (particles/mL)	1.82×10^{11}	8.08×10^{10}	2.46×10^{11}	1.19×10^{11}
IC_{50} (particles/mL)	8.35×10^{11}	6.80×10^{11}	not reached	not reached
95% IC	$5.8\text{-}12.5 \times 10^{11}$	$4.46\text{-}11.59 \times 10^{11}$	–	–

Concentration–response curves were fitted using a three-parameter log (inhibitor vs. normalised response model).

CRediT authorship contribution statement

Verónica Moreno-Martín: Writing – original draft, Visualization, Methodology, Investigation, Formal analysis, Data curation, Conceptualization. **Maria López:** Writing – review & editing, Investigation. **Cristian Roldan:** Methodology, Formal analysis, Data curation. **David Bou:** Methodology, Formal analysis, Data curation. **Sonia Fraga:** Writing – review & editing, Investigation, Formal analysis, Conceptualization. **João Paulo Teixeira:** Writing – review & editing. **Ana López-Lilao:** Writing – original draft, Supervision, Methodology, Data curation, Conceptualization. **Vicenta Sanfélix:** Supervision, Resources, Conceptualization. **Raúl Moliner:** Writing – original draft. **Eliseo Monfort:** Writing – review & editing, Supervision, Resources, Conceptualization. **Mar Viana:** Writing – review & editing, Supervision, Resources, Methodology, Conceptualization.

Funding sources

Life NanoHealth (LIFE20 ENV-ES-000187)
GAIA-IVACE (IMAMCA/2023/1)

Declaration of competing interest

The authors declare that they have no known competing financial interests or personal relationships that could have appeared to influence the work reported in this paper.

Acknowledgements

This work was carried out in the framework of project LIFE-NanoHealth (LIFE20 ENV-ES-000187). It was also supported by the Spanish Ministry of Science and Innovation (Project CEX2018-000794-S), by the Government of Catalonia Agency for Administration of University and Research Grants (AGAUR) (project 2017 SGR41) and by the Government of Valencia (GAIA-IVACE)(IMAMCA/2023/1).

Appendix A. Supplementary data

Supplementary data to this article can be found online at https://doi.org/10.1016/j.jaerosci.2024.106485.

Data availability

Data will be made available on request.

References

Aparicio Sanchez, J., & Baena Molina, E. (2013). *Manual de actualización en materiales y técnicas de colocación de recubrimientos cerámicos, 1*, 234–240.
Asbach, C., Kuhlbusch, T., Kaminski, H., Stahlmecke, B., Plitzko, S., Götz, U., … Dahmann, D. (2012). Standard Operation Procedures for assessing exposure to nanomaterials, following a tiered approach. *NanoGEM*, 5–7.
Barba, A. (2002). *Materias Primas para la Fabricación de Soportes de Baldosas Cerámicas (Raw Materials for Manufacturing Floor and Wall Tiles)*. Instituto de Tecnología Cerámica.
Bessa, M. J., Brandão, F., Viana, M., Gomes, J. F., Monfort, E., Cassee, F. R., Fraga, S., & Teixeira, J. P. (2020). Nanoparticle exposure and hazard in the ceramic industry: An overview of potential sources, toxicity and health effects. *Environmental Research, 184*. https://doi.org/10.1016/j.envres.2020.109297
Black, I., & Chua, K. L. (2017). Laser cutting of thick ceramic tile. *Optics & Laser Technology, 29*, 193–205.
Bolyard, S. C., Reinhart, D. R., & Santra, S. (2013). Behavior of engineered nanoparticles in landfill leachate. *Environ Sci Technol, 47*, 8114–8122. https://doi.org/10.1021/es305175e
Bramming Jørgensen, R., & Teresia Kero, I. (2017). Real-time measurements and characterization of airborne particulate matter from a primary silicon carbide production plant. https://doi.org/10.3390/ijerph14121611.
Carlo, R. V., Sheehy, J., Feng, H. A., & Sieber, W. K. (2010). Journal of occupational and environmental hygiene laboratory evaluation to reduce respirable crystalline silica dust when cutting concrete roofing tiles using a masonry saw laboratory evaluation to reduce respirable crystalline silica dust when cutting concrete roofing tiles using a laboratory evaluation to reduce respirable crystalline silica dust when cutting concrete roofing tiles using a masonry saw. *Journal of Occupational and Environmental Hygiene, 7*, 245–251. https://doi.org/10.1080/15459620903579695
Cerame Unie (The European Ceramic Industry Association). (2021). *Ceramics – a continental champion, 6*. Ceramic Roadmap. to 2050.
Davoren, M., Herzog, E., Casey, A., Cottineau, B., Chambers, G., Byrne, H. J., & Lyng, F. M. (2007). In vitro toxicity evaluation of single walled carbon nanotubes on human A549 lung cells. *Toxicology in Vitro, 21*, 438–448. https://doi.org/10.1016/j.tiv.2006.10.007
De Ipiña, J. M. L., Vaquero, C., Boutry, D., Damlencourt, J. F., Neofytou, P., Pilou, M., Jankowska, E., Larraza, I., Pina, R., Fernández, S., Contreras, S., Romero, A., Calderon, M., Swiezewsk, P., Otkallo, K., Pintea, A., Salazar, C., Oroz, T., Hargreaves, B., … Thompson, D. (2015). Strategies, methods and tools for managing nanorisks in construction. In *Journal of physics: Conference series*. Institute of Physics Publishing. https://doi.org/10.1088/1742-6596/617/1/012035.
Duan, H., Li, J., & Liu, G. (2017). Growing threat of urban waste dumps. *Nature, 546*, 599. https://doi.org/10.1038/546599b
Fonseca, A. S., Viana, M., Querol, X., Moreno, N., de Francisco, I., Estepa, C., & de la Fuente, G. F. (2015). Workplace exposure to precess-generated ultrafine and nanoparticles in ceramic processes using laser technology. Indoor and Outdoor Nanoparticles. *The hadbook of environmental chemistry, 48*, 159–179. https://doi.org/10.1007/698_2015_422

Fonseca, A. S., Maragkidou, A., Viana, M., Querol, X., Hämeri, K., de Francisco, I., Estepa, C., Borrell, C., Lennikov, V., & de la Fuente, G. F. (2015a). Process-generated nanoparticles from ceramic tile sintering: Emissions, exposure and environmental release. *Science of the Total Environment, 565*, 922–932. https://doi.org/10.1016/j.scitotenv.2016.01.106

Fonseca, A. S., Viana, M., Querol, X., Moreno, N., de Francisco, I., Estepa, C., & de la Fuente, G. F. (2015b). Ultrafine and nanoparticle formation and emission mechanisms during laser processing of ceramic materials. *Journal of Aerosol Science, 88*, 48–57. https://doi.org/10.1016/j.jaerosci.2015.05.013

Garcia, A., Jones, E., Echt, A. S., & Hall, R. M. (2014). An evaluation of an aftermarket local ExhaustVentilation device for suppressing respirable dust and respirable crystalline silica dust from powered saws. *Journal of Occupational and Environmental Hygiene, 11*(11), 200–207. https://doi.org/10.1080/15459624.2014.955182

Hall, R. M., Achutan, C., Sollberger, R., Robert, E. M., & Rodriguez, M. (2013). Exposure assessment for roofers exposed to silica during installation of roof tiles. *Journal of Occupational and Environmental Hygiene, 10*. https://doi.org/10.1080/15459624.2012.739439

Hall, S., Stacey, P., Pengelly, I., Stagg, S., Saunders, J., & Hambling, S. (2022). Characterizing and comparing emissions of dust, respirable crystalline silica, and volatile organic compounds from natural and artificial stones. *Ann Work Expo Health, 66*, 139–149. https://doi.org/10.1093/annweh/wxab055

Hossain, S. S., Son, H. J., Park, S., & Bae, C. J. (2023). Extrusion-based 3D printing alumina-silica inks: Adjusting rheology and sinterability incorporating waste derived nanoparticles. *Journal of the European Ceramic Society, 43*, 4865–4876. https://doi.org/10.1016/J.JEURCERAMSOC.2023.03.068

Ivask, A., Titma, T., Visnapuu, M., Vija, H., Käkinen, A., Sihtmäe, M., … Kahru, A. (2015). Toxicity of 11 metal oxide nanoparticles to three mammalian cell types in vitro. Curr. Top. Med. Chem. 15 (18), 1914-1929. doi:10.2174/1568026615666150506150109. PMID: 25961521.

Krajcarz, D., Bańkowski, D., & Młynarczyk, P. (2017). The effect of traverse speed on kerf width in AWJ cutting of ceramic tiles. In *Procedia engineering* (pp. 469–473). Elsevier Ltd. https://doi.org/10.1016/j.proeng.2017.06.081.

Lelieveld, J., Evans, J. S., Fnais, M., Giannadaki, D., & Pozzer, A. (2015). The contribution of outdoor air pollution sources to premature mortality on a global scale. https://doi.org/10.1038/nature15371.

López, M., López Lilao, A., Ribalta, C., Martínez, Y., Piña, N., Ballesteros, A., Fito, C., Koehler, K., Newton, A., Monfort, E., & Viana, M. (2022). Particle release from refit operations in shipyards: Exposure, toxicity and environmental implications. *Science of the Total Environment, 804*, Article 150216. https://doi.org/10.1016/j.scitotenv.2021.150216

Lovén, K., Isaxon, C., Ahlberg, E., Bermeo, M., Messing, M. E., Kåredal, M., Hedmer, M., & Rissler, J. (2023). Size-resolved characterization of particles >10 nm emitted to air during metal recycling. *Environment International, 174*, Article 107874. https://doi.org/10.1016/j.envint.2023.107874

Martínez, G., Merinero, M., Pérez-Aranda, M., Pérez-Soriano, E. M., Ortiz, T., Begines, B., & Alcudia, A. (2021). Environmental impact of nanoparticles' application as an emerging technology: A review. *Materials*. https://doi.org/10.3390/ma14010166

Oberdörster, G. (2001). Pulmonary effects of inhaled ultrafine particles. *International Archives of Occupational and Environmental Health, 74*, 1–8.

Pampuch, R. (2014). *An introduction to ceramics* (1st ed.). Springer.

Pope III, C. A., & Dockery, D. W. (2006). Health effects of fine particulate air pollution : Lines that connect health effects of fine particulate air pollution : Lines that connect. *Journal of air & waste management association, 56*, 709–742. https://doi.org/10.1080/10473289.2006.10464485

Querol, X., Alastuey, es, Rodriguez, S., Ruiz, C. R., Cots, N., Massagu, G., & Puig, O. (2001). Atmospheric environment. *PM10 and PM2.5 source apportionment in the Barcelona Metropolitan area, Catalonia, Spain, 35*, 6407–6419. n.d.

Querol, X., Whateley, M. K. G., Fernfindez-Turiel, J. L., & Tuncali, E. (1997). Geological controls on the mineralogy and geochemistry of the Beypazari lignite, central Anatolia, Turkey. *International Journal of Coal Geology, 33*(3), 255–271. https://doi.org/10.1016/S0166-5162(96)00044-4.

Rafieepou, A., Azari, M. R., & Khodagholi, F. (2023). Cytotoxic effects of crystalline silica in form of micro and nanoparticles on the human lung cell line A549. *Toxicology and Industrial Health, 39*, 23–25.

Rakshit, R., & Das, A. K. (2019). A review on cutting of industrial ceramic materials. *Precision Engineering*. https://doi.org/10.1016/j.precisioneng.2019.05.009

Ribalta, C., López-Lilao, A., Estupiñá, S., Fonseca, A. S., Tobías, A., García-Cobos, A., … Viana, M. (2019a). Health risk assessment from exposure to particles during packing in working environments. *Science of the Total Environment, 671*, 474–487. https://doi.org/10.1016/j.scitotenv.2019.03.347

Ribalta, C., Viana, M., López-Lilao, A., Estupiñá, S., Minguillón, M. C., Mendoza, J., Díaz, J., Dahmann, D., & Monfort, E. (2019b). On the relationship between exposure to particles and dustiness during handling of powders in industrial settings. *Ann Work Expo Health, 63*, 107–123. https://doi.org/10.1093/annweh/wxy092

Salmatonidis, A., Viana, M., Pérez, N., Alastuey, A., de la Fuente, G. F., Angurel, L. A., Sanfélix, V., & Monfort, E. (2018). Nanoparticle formation and emission during laser ablation of ceramic tiles. *Journal of Aerosol Science, 126*, 152–168. https://doi.org/10.1016/j.jaerosci.2018.09.006

Salmatonidis, A., Ribalta, C., Sanfélix, V., Bezantakos, S., Biskos, G., Vulpoi, A., Simion, S., Monfort, E., & Viana, M. (2019). Workplace exposure to nanoparticles during thermal spraying of ceramic. *Coatings, 63*, 91–106. https://doi.org/10.1093/annweh/wxy094

Salmatonidis, A., Viana, M., Biskos, G., & Bezantakos, S. (2020). Particle size distributions and hygroscopic restructuring of ultrafine particles emitted during thermal spraying. *Aerosol Science and Technology, 54*, 1359–1372. https://doi.org/10.1080/02786826.2020.1784837

Sebaugh, J. L. (2011). Guidelines for accurate EC50/IC50 estimation. *Pharmaceutical Statistics, 10*, 128–134. https://doi.org/10.1002/pst.426

Tokgun, O., Demiray, A., Kaya, B., Karagür, E. R., Demir, E., Burunkaya, E., & Akça, H. (2015). Silica nanoparticles can induce apoptosis via dead receptor and caspase 8 pathway on A549 cells. *Advances in Food Sciences, 37*, 65–70.

Tsai, S. J., Ada, E., Isaacs, J. A., & Ellenbecker, M. J. (2009). Airborne nanoparticle exposures associated with the manual handling of nanoalumina and nanosilver in fume hoods. *Journal of Nanoparticle Research, 11*, 147–161. https://doi.org/10.1007/s11051-008-9459-z

Viana, M., Fonseca, A. S., Querol, X., López-Lilao, A., Carpio, P., Salmatonidis, A., & Monfort, E. (2017). Workplace exposure and release of ultrafine particles during atmospheric plasma spraying in the ceramic industry. *Science of the Total Environment, 599–600*, 2065–2073. https://doi.org/10.1016/j.scitotenv.2017.05.132

Viitanen, A.-K., Uuksulainen, S., Koivisto, A. J., Hämeri, K., & Kauppinen, T. (2017). Workplace measurements of ultrafine particles-A literature review. *Ann Work Expo Health, 61*, 749–758. https://doi.org/10.1093/annweh/wxx049

Voliotis, A., Bezantakos, S., Giamarelou, M., Valenti, M., Kumar, P., & Biskos, G. (2014). Nanoparticle emissions from traditional pottery manufacturing. https://doi.org/10.1039/c3em00709j.

WHS. (2023). *Meeting of workplace relations and work health and safety ministers (WHS)*.

Xu, Y., Wang, J., & Yang, Z. (2023). Generic goal-oriented design for layout and cutting of floor tiles. *Automation in Construction, 152*. https://doi.org/10.1016/j.autcon.2023.104903